In Silico Evaluation of Temperature and Geometrical Parameters on Material Extrusion 3D Printing

Sidonie F. Costa [1,*], Fernando M. Duarte [2], and José A. Covas [2]

[1] CIICESI—Escola Superior de Tecnologia e Gestão, Politécnico do Porto, Felgueiras, Portugal
[2] Institute for Polymers and Composites (IPC), Department of Polymer Engineering, University of Minho, Guimarães, Portugal
Email: sfc@estg.ipp.pt (S.F.C.); fduarte@dep.uminho.pt (F.M.D.); jcovas@dep.uminho.pt (J.A.C.)
*Corresponding author

***Abstract*—Additive Manufacturing (AM), particularly through material extrusion techniques such as Fused Filament Fabrication (FFF), has gained significant practical importance due to the ability to create customized complex geometries without molds. However, FFF is influenced by numerous parameters that affect the mechanical performance, surface quality and dimensional accuracy of printed parts. For example, effective bonding between filaments, which is essential for mechanical properties, depends on factors such as extrusion velocity and temperature, and part geometry. This study uses a computational tool that predicts temperature and bonding development in a 3D object created via FFF to investigate the impact of geometrical factors on filament bonding. The results showed that filament bonding is little affected by part dimensions except for narrow widths and small heights, i.e., geometrical factors are important at small scales. Additionally, increasing extrusion and/or environment temperatures enhance interlayer bonding quality, although the latter has a much smaller influence.**

***Keywords*—3D printing, material extrusion, fused filament fabrication, heat transfer, bonding**

I. Introduction

Material Extrusion (ME) 3D printing involves the layer-by-layer construction of 3D objects from a digital model, utilizing filaments of thermoplastic materials or composites [1, 2]. Unlike conventional manufacturing methods, 3D printing does not require molds, thereby reducing production time and costs, while enabling the creation of complex geometries with minimal material waste [3, 4]. This flexibility accelerates prototyping, enhancing product development cycles and competitive edge [5, 6]. Moreover, emerging methodologies like bioprinting and 4D printing have expanded the horizons within the medical domain, offering novel avenues for exploration and application [7].

Fused Filament Fabrication (FFF), a major ME 3D printing technique, involves a series of stages, including heating, melting, flow, bonding, and solidification/cooling processes [8, 9]. Consequently, numerous parameters affect significantly the quality and reliability of printed parts, particularly mechanical performance, surface finish, and dimensional tolerances [10–12]. For example, Li *et al.* [13] found that tensile strength is closely linked to the degree of interface bonding, while Attolico *et al*. [14] demonstrated the impact of extrusion temperature on the orthotropic mechanical behavior under quasi-static tensile loads. The role of bonding between filaments on the performance of 3D printed parts has been extensively discussed [15–19]. The molecular diffusion required for bonding depends on the rheological properties of the polymer, which in turn are influenced by local temperatures during filament deposition and cooling. Since the process involves significant temperature gradients, the resulting stresses may cause warpage and delamination [20]. In this context, Striemann *et al.* [21] demonstrated the potential of thermal management to enhance the mechanical properties of FFF parts, by keeping the interlayer zone temperature above the glass transition temperature during the deposition stage, resulting in a 15% increase in tensile strength.

Due to the practical importance of the topic, several models have been developed to predict temperature evolution and bonding outcomes in ME 3D printing. Initial models considered the cooling of a single filament due to convection [15, 22], while subsequent efforts introduced the effects of filament contact and presence of voids between filaments [20, 23–25]. Experimental methods to predict temperatures in FFF have also been proposed, despite the challenging task of obtaining accurate measurements. Bragg grating sensors [26] and infrared thermography [27] have been utilized to measure temperature evolution, providing valuable data to validate the theoretical models.

This study aims at assessing in silico the influence of geometrical factors of parts to be 3D printed on filament bonding, an obviously important subject that has been largely ignored in open literature. Extrusion and

Manuscript received July 10, 2024; revised July 30, 2024; accepted August 10, 2024; published June 17, 2025.

environment temperatures were also varied to yield a better understanding of possible correlations between geometrical parameters and operating conditions.

II. Modeling ME 3D Printing

As discussed in detail elsewhere [23], during the deposition stage in FFF several heat transfer phenomena occur simultaneously, including conduction along the filaments and through their cross-section, heat losses by convection and radiation to the surrounding air, and conduction with adjacent filaments and the machine's printing bed. The authors have previously performed an energy balance, which was translated into a differential equation describing the global heat transfer process [28]. The solution to the latter, together with an algorithm that automatically defines and updates contacts as deposition progresses, as well as a healing criterion, yields the temperature development and the degree of bonding between adjacent filaments for any 3D printed part [29]. The predictions closely matched experimental data [16]. The model was further improved to consider the existence of filaments of varying lengths, which enabled to include the effect of build orientation on bonding [30]. Parameters such as process temperatures, infill density, deposition sequence and deposition velocity are taken in. Fig. 1 presents a general flowchart of the computer code. Although some of the assumptions made have been relaxed in more recent thermal models, the code is still one of the few providing experimentally validated predictions of temperature histories and degree of bonding for all part locations [31, 32].

Fig. 2 illustrates the complex (and somewhat surprising) interrelationship between bonding and thermal contact conductance between two adjacent filaments. If bonding between these does not occur (due to insufficient time at sufficiently high temperatures), heat transfer is limited, causing them to cool slower. Unexpectedly, this can favor bonding between filaments in subsequent layers, as higher temperatures are retained. However, as this bonding strengthens, heat transfer increases, resulting in higher cooling rates. In turn, this more efficient cooling hinders bonding in the succeeding layers. This cyclic mechanism emphasizes the dynamic nature of bonding.

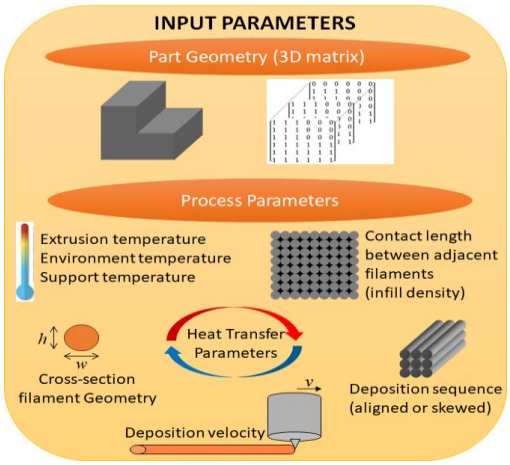

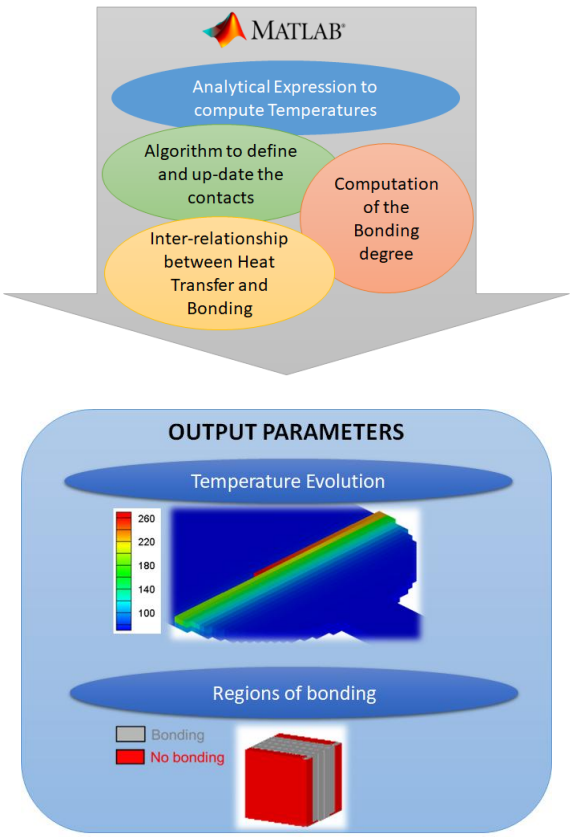

Fig. 1. General flowchart of the computer model.

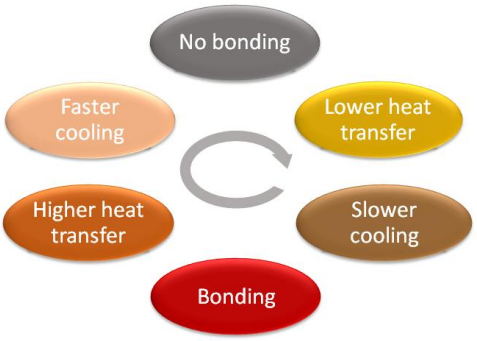

Fig. 2. Correlation between bonding and heat transfer.

III. In Silico Experiments

A. Part geometry and Material

A simple cube with dimensions 30×30×30 mm was assumed as the reference part. As illustrated in Fig. 3 (a), the cube was made to "grow" either vertically or horizontally, resulting in the creation of six distinct parts, denoted as H60, H90, H120, W60, W90, and W120. When the cube grows vertically, the number of layers obviously increases, but the thermal conditions remain identical. Conversely, expanding the cube horizontally maintains the number of layers but increases the number of filaments per layer. Thus, at constant extrusion velocity, more time is needed to print each layer, delaying

contacts points and potentially impacting on temperatures, thereby affecting bonding.

Consequently, widening a part should exert a greater influence on the degree of bonding, than making it taller. As shown in Fig. 3 (b), the cube was also made to "shrink" either vertically or horizontally, resulting in six further parts, denoted as H18, H6, H1.5, W18, W6, and W1.5.

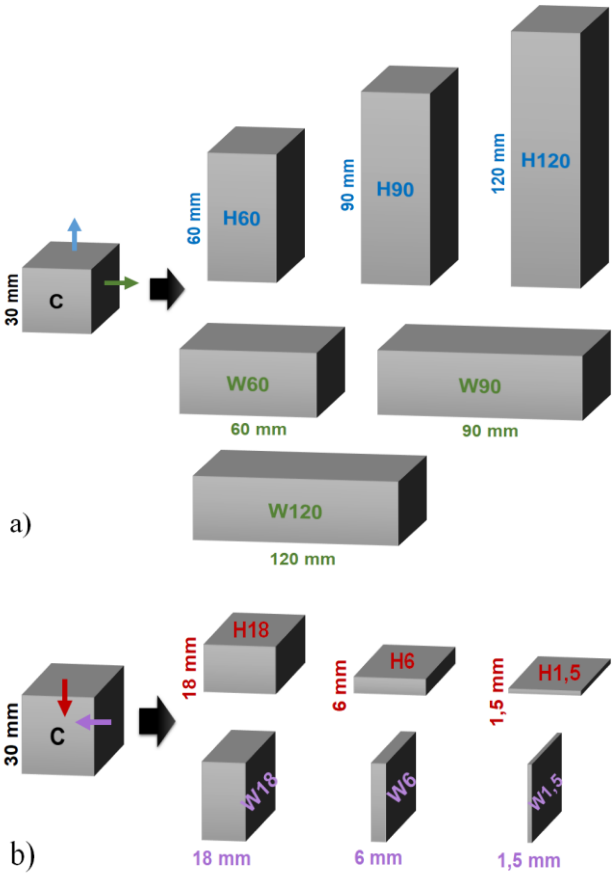

Fig. 3. Changing the dimensions of the reference cube (a) vertical and horizontal growth; (b) vertical and horizontal shrinkage (dimensions and nomenclature are indicated).

ABS P400 material (often used in ME 3D printing) is considered, with the properties presented in Table I. An expression for the welding time (necessary to compute the degree of bonding) was obtained from the literature [29].

TABLE I. ABS P400 PROPERTIES

Property	Value
Density (kg/m^3), ρ	1050
Thermal conductivity (W/m^{2}ºC), k	0.18
Specific heat (J/kg ºC), C	2020

B. Process and Computational Parameters

Tables II and III show the reference (and often adopted in practice) printing parameters and computational variables, respectively.

TABLE II. REFERENCE PRINTING PARAMETERS AND HEAT TRANSFER COEFFICIENTS

Property	Value
Extrusion Temperature, T_L (ºC)	270
Environment Temperature, T_E (ºC)	70
Printing Bed Temperature, T_{sup} (ºC)	70
Extrusion Velocity, v (m/s)	0.025
Convective heat transfer coefficient, h_{conv} (W/m^2•ºC)	65
Thermal contact conductance between adjacent filaments, h_i (W/m^2•ºC)	$h_i \in [10^{-4};220]$
Thermal contact conductance between filaments and support, h_{sup} (W/m^2•ºC)	10
Infill Density (%)	100
Filament cross-section width, w (mm)	0.3
Filament cross-section height, h (mm)	0.3
Deposition Sequence	Unidirectional and Aligned

TABLE III. COMPUTATIONAL PARAMETERS

Property	Value
Time increment, t_i (s)	0.1
Temperature convergence error, ε (ºC)	1

Table IV indicates the number of filaments, as well as the manufacturing and computation times (on a PC) associated with each geometry. At each time increment along the filament deposition, all conditions are saved, updated, and temperatures are computed using a convergent iterative method due to the thermal contacts between filaments. Consequently, extensive 3D matrices are required, demanding a significant number of computations. For instance, considering a part comprised of 10,000 filaments (the reference cube), 299,820 thermal conditions must be defined and updated, which justifies the substantial computation times involved.

TABLE IV. NUMBER OF FILAMENTS AND MANUFACTURING / COMPUTATION TIMES

Dimensions (mm)	Number of filaments	Real Manufacturing Time (h)	Computation Time (h)
30×30×30 (C)	10,000	3.3	12
30×30×60 (H60)	20,000	6.7	30
30×30×90 (H90)	30,000	10	50
30×30×120 (H120)	40,000	13.3	60
30×60×30 (W60)	20,000	6.7	50
30×90×30 (W90)	30,000	10	80
30×120×30 (W120)	40,000	13.3	180

IV. RESULTS AND DISCUSSION

A. Vertical and Horizontal Increase of the Cube

Taking into account the input data from Tables I to III, both the reference cube and parts H60, H90, H120, W60, W90 and W120 are predicted to show good bonding quality. However, if the extrusion temperature is reduced by 20 ºC (from 270 ºC to 250 ºC), the bonding volume

(i.e., the percentage of the part volume exhibiting good bonding quality) will begin to be compromised. As seen in Fig. 4(a), regions lacking bonding become apparent at the bottom layers, due to contact with the (cooler) printing bed.

As depicted in Fig. 4(b), a further reduction of 5 ºC in the extrusion temperature results in a reduction in the bonding volume to approximately 65–67%. Minimal differences in quality between the parts are observed. As for the location of regions without bonding, they appear at the edges of the parts. Fig. 5 displays the temperatures of four adjacent filaments at three instants during deposition. As the extrusion head returns to the initial *xx* position, the temperature differences between the two filaments increase, hindering bonding.

If the extrusion temperature is reduced to 240 ºC, a significant deterioration in bonding quality is predicted (Fig. 4(c), thus emphasizing the importance of selecting a sufficiently high extrusion temperature for good quality bonding [14]. The effects of this process parameter and of increasing the height/width of the part are clearly seen in Fig. 4(d), which relates bonding volume with extrusion temperature for the various parts. Differences in bonding are within 6%.

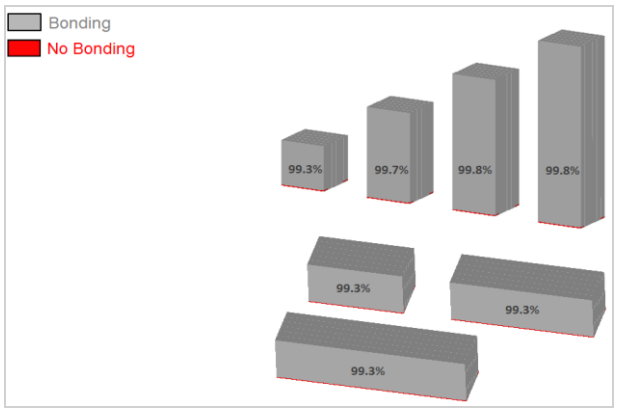

(a)

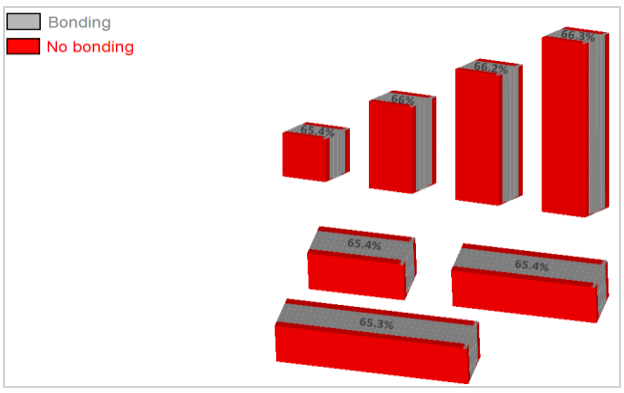

(b)

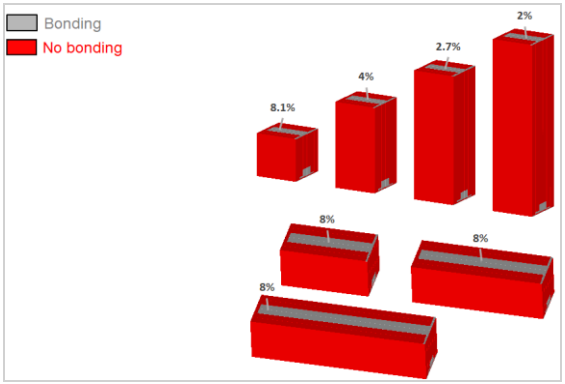

(c)

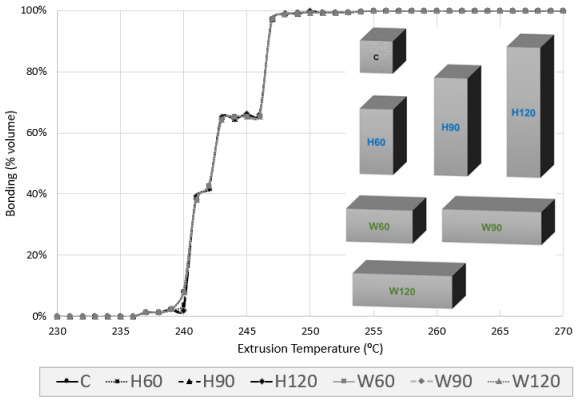

(d)

Fig. 4. Bonding volume (%) for parts C, H60, H90, H120, W60, W90, and W120, considering: (a) T_L = 250 ºC; (b) T_L = 245 ºC; (c) T_L = 240 ºC; (d) 230 ºC ≤ T_L ≤ 270 ºC.

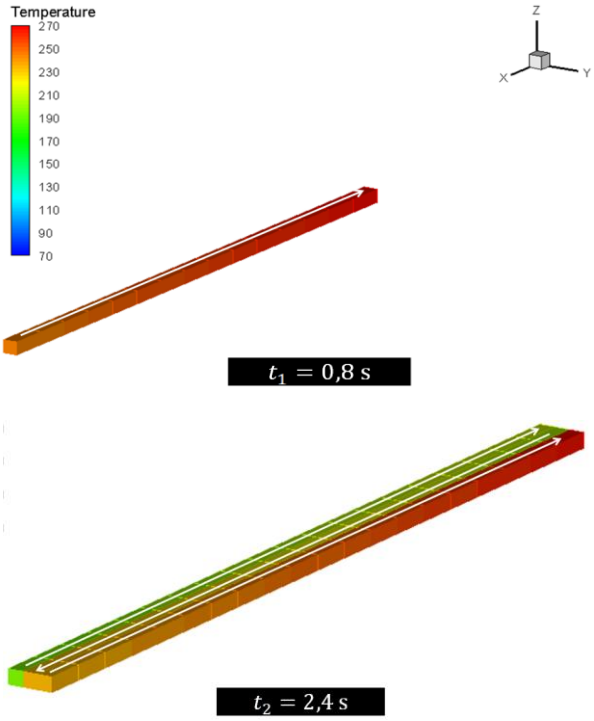

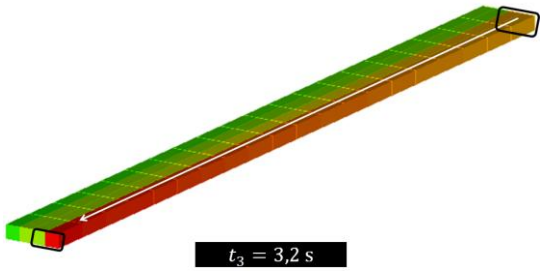

Fig. 5. Temperatures of four adjacent filaments at three instants during deposition.

Similarly, Fig. 6 illustrates the effect of the environment temperature on bonding. This temperature can be changed and controlled in 3D printers fitted with an oven. At constant extrusion temperature (270 ºC), regions with bonding appear for environment temperatures above 30 ºC, with 100% bonding being reached when that temperature attains 55 ºC (Fig. 6(a)). The maximum difference in bonding for the various geometries is less than 7%. Figs. 4(d) and 6(a) show that (1) extrusion and environment temperatures significantly impact on bonding, a result that has been corroborated experimentally [14, 33]; (2) extrusion temperature exerts a greater effect; (3) the correlation between bonding volume and extrusion/environment temperature is non-linear.

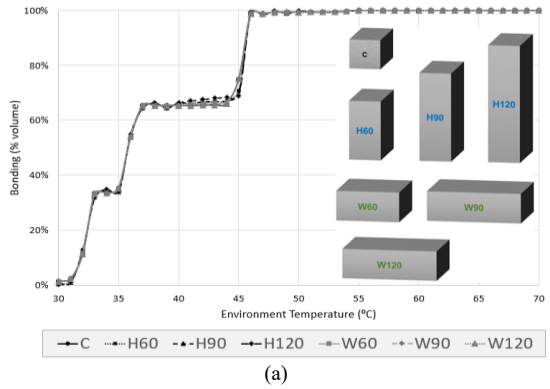

(a)

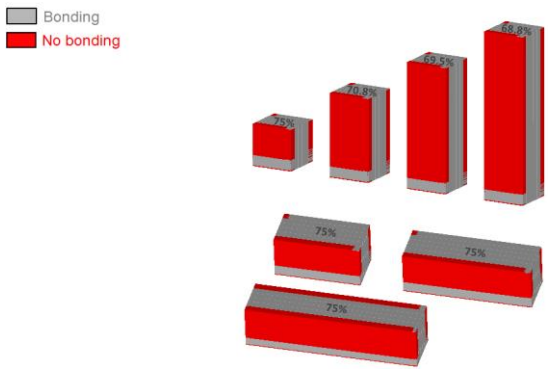

(b)

Fig. 6. Influence of the Environment Temperature (ºC) on bonding (%), for parts C, H60, H90, H120, W60, W90, and W120, considering: (a) 30 ºC ≤ T_E ≤ 70 ºC; (b) T_E = 45 ºC.

Assuming an environment temperature of 45ºC Fig. 6(b), the initial (bottom) layers show no bonding, followed by a few well bonded layers, then more non-bonded layers until the top layer. This results from the heat transfer dynamics illustrated in Fig. 2. Initially, inadequate bonding occurs due to contact with the printing bed; this limits heat transfer between adjacent filaments and slows their cooling, thus promoting bonding in the subsequent layers. However, once bonding happens, heat transfer improves, cooling rates increase and bonding in the next layers is hindered.

B. Vertical and Horizontal Decrease of the Cube

Fig. 7 shows the effect of extrusion temperature on the bonding volume when the reference cube decreases in size horizontally or vertically. In the first case Fig. 7(a) the results are similar for all parts, except for the thinnest one with a notably higher bonding volume. This part is 1.5 mm thin, corresponding to 5 filaments and requiring only 6 s to complete each layer, i.e., adjacent filaments are hotter and thus have a tendency to bond well. Achieving 100% bonding is observed at 250 ºC for this part and at 255 ºC for the remaining.

Respecting the vertical decrease, the behavior depicted in Fig. 7(b) is different. The response of part H18 is similar to that of the reference cube, H6 shows some differences, while the profile of H1.5 is dissimilar. As the extrusion temperature increases, initially the bonding volumes for parts H6 and H1.5 are higher than the remaining due to the contact with the printing bed and the small number of layers. Subsequently, the curves intersect and the bonding volumes of parts H6 and H1.5 become lower. For parts with fewer layers, contact with the printing bed plays a crucial role in heat transfer, initially compensating for low extrusion temperatures but ultimately hindering bonding as the extrusion temperature rises, since there are not enough additional layers to offset cooling from contact with the printing bed.

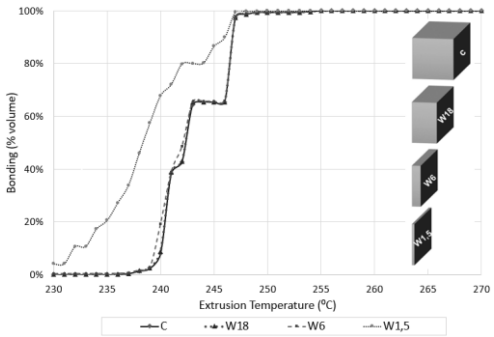

(a)

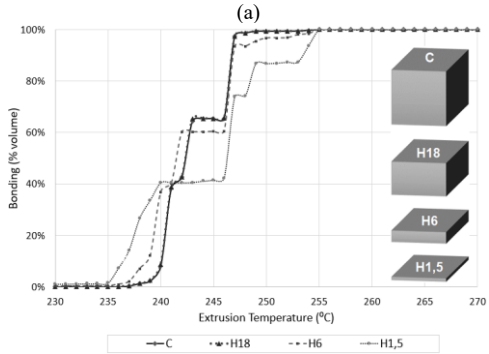

(b)

Fig. 7. Influence of the Extrusion Temperature (ºC) on bonding (%) for parts a) C, W18, W6 and W1.5; b) C, H18, H6 and H1.5.

V. Conclusions and Future Work

The impact of geometrical parameters, together with extrusion and environment temperature, on filament bonding in Fused Filament Fabrication (FFF) was investigated in silico.

High extrusion and environment temperatures significantly enhance filament bonding, although a 20 ºC variation in the latter is needed to achieve the effect of a 10 ºC change in the former.

In general, variations in part height or width offered minimal influence on bonding, suggesting little effect on the heat transfer dynamics. However, for narrow widths and heights (1.5 mm), the bonding volume was markedly altered, suggesting effects at the small scale.

Future work will focus on refining the modeling code utilized and apply it to further clarify the role of the main process and material parameters on the performance of 3D printed parts.

Conflict of Interest

The authors declare no conflict of interest.

Author Contributions

Sidonie F. Costa selected the case study, performed the computations and wrote a first draft of the manuscript. Fernando M. Duarte and José A. Covas contributed to the final manuscript. All co-authors designed the research and discussed the results. All authors had approved the final version.

Funding

This work has been partially supported by national funds through FCT—Fundação para a Ciência e Tecnologia through project UIDB/04728/2020.

Partial support for this research has been provided by the Search-ON2: Revitalization of HPC infrastructure of Uminho, (NORTE-07-0162-FEDER-000086), co-funded by the North Portugal Regional Operational Programme (ON.2-O Novo Norte), under the National Strategic Reference Framework (NSRF), through the European Regional Development Fund (ERDF).

References

[1] C. K. Chua, K. F. Leong, and C. S. Lim, *Rapid Prototyping: Principles and Applications*, 3rd ed. Singapore: World Scientific, 2010.

[2] S. H. Siddique, P. J. Hazell, H. Wang, J. P. Escobedo, and A. A. H. Ameri, "Lessons from nature: 3D printed bio-inspired porous structures for impact energy absorption—A review," *Addit. Manuf.*, vol. 58, 103051, 2022. doi: 10.1016/j.addma.2022.103051

[3] L. Zhou, J. Miller, J. Vezza, M. Mayster, M. Raffay, Q. Justice, Z. Al Tamimi, G. Hansotte, L. D. Sunkara, and J. Bernat, "Additive manufacturing: A comprehensive review," *Sensors*, vol. 24, no. 9, 2668, 2024. doi: 10.3390/s24032668

[4] M. Jayakrishna, M. Vijay, and B. Khan, "An overview of extensive analysis of 3D printing applications in the manufacturing sector," *J. Eng.*, 7465737, 2023. doi: 10.1155/2023/7465737

[5] D. S. Ingole, A. M. Kuthe, S. B. Thakare, and A. S. Talankar, "Rapid prototyping—A technology transfer approach for development of rapid tooling," *Rapid Prototyp. J.*, vol. 15, no. 4, pp. 280–290, 2009. doi: 10.1108/13552540910979794

[6] S. F. Iftekar, A. Aabid, A. Amir, and M. Baig, "Advancements and limitations in 3D printing materials and technologies: A critical review," *Polymers,* vol. 15, no. 11, 2519, 2023. doi: 10.3390/polym15112519

[7] K. Deshmukh, M. T. Houkan, and M. A. A. AlMaadeed, "Introduction to 3D and 4D printing technology: State of the art and recent trends," in *3D and 4D Printing of Polymer Nanocomposite Materials: Processes, Applications, and Challenges*, Amsterdam, The Netherlands: Elsevier, 2019, pp. 1–24.

[8] M. E. Mackay, "The importance of rheological behavior in the additive manufacturing technique material extrusion," *J. Rheol.*, vol. 62, no. 6, pp. 1549–1561, 2018. doi: 10.1122/1.5037687

[9] A. A. Rashid and M. Koç, "Fused filament fabrication process: A review of numerical simulation techniques," *Polymers*, vol. 13, no. 20, 3534, 2021. doi: 10.3390/polym13203534

[10] A. M. Abdelrhman, W. W. Gan, and D. Kurniawan, "Effect of part orientation on dimensional accuracy, part strength, and surface quality of three dimensional printed part," *IOP Conf. Ser.: Mater. Sci. Eng.*, vol. 694, pp. 12–48, 2019. doi: 10.1088/1757-899X/694/1/012048

[11] S. Hwang, E. I. Reyes, K. Moon, R. C. Rumpf, and N. S. Kim, "Thermo-mechanical characterization of metal/polymer composite filaments and printing parameter study for fused deposition modeling in the 3D printing process," *J. Electron. Mater.*, vol. 44, no. 3, pp. 771–777, 2015. doi: 10.1007/s11664-014-3425-6

[12] O. E. Akbaş, O. Hıra, S. Z. Hervan, S. Samankan, and A. Altınkaynak, "Dimensional accuracy of FDM-printed polymer parts," *Rapid Prototyp. J.*, vol. 26, no. 2, pp. 288–298, 2019. doi: 10.1108/RPJ-04-2019-0115

[13] H. Li, T. Wang, J. Sun, and Z. Yu, "The effect of process parameters in fused deposition modelling on bonding degree and mechanical properties," *Rapid Prototyp. J.*, vol. 24, no. 1, pp. 80–92, 2018. doi: 10.1108/RPJ-06-2016-0097

[14] M. A. Attolico, C. Casavola, A. Cazzato, V. Moramarco, and G. Renna, "Effect of extrusion temperature on fused filament fabrication parts orthotropic behaviour," *Rapid Prototyping Journal*, vol. 26, no. 4, pp. 639–647, 2020. doi: 10.1108/RPJ-06-2019-0163

[15] M. A. Yardimci, H. Takeshi, S. Güceri, and S. C. Danforth, "Thermal analysis of fused deposition," in *Proc. in Solid Freeform Fabrication Symposium*, Austin, TX, 1997, pp. 689–698.

[16] S. F. Costa, F. M. Duarte, and J. A. Covas, "Estimation of filament temperature and adhesion development in fused deposition techniques," *J. Mater. Process. Technol.*, vol. 245, pp. 167–179, 2017. doi: 10.1016/j.jmatprotec.2017.02.026

[17] D. Bhalodi, K. Zalavadiya, and P. K. Gurrala, "Influence of temperature on polymer parts manufactured by fused deposition modeling process," *J. Braz. Soc. Mech. Sci. Eng.*, vol. 41, 113, 2019. doi: 10.1007/s40430-019-1616-z

[18] S. Charlon, J. L. Boterff, and J. Soulestin, "Fused filament fabrication of polypropylene: Influence of the bead temperature on adhesion and porosity," *Addit. Manuf.*, vol. 38, 101838, 2021. doi: 10.1016/j.addma.2021.101838

[19] M. H. Sehhat, A. Mahdianikhotbesara, and F. Yadegari, "Impact of temperature and material variation on mechanical properties of parts fabricated with Fused Deposition Modeling (FDM) additive manufacturing," *Int. J. Adv. Manuf. Technol.*, vol. 120, pp. 4791–4801, 2022. doi: 10.1007/s00170-022-09043-0

[20] N. Rudolph, J. Chen, and T. Dick, "Understanding the temperature field in fused filament fabrication for enhanced mechanical part performance," *AIP Conference Proceedings*, vol. 2055, 140003, 2019. doi: 10.1063/1.5084906

[21] P. Striemann, D. Hülsbusch, M. Niedermeier, and F. Walther, "Optimization and quality evaluation of the interlayer bonding performance of additively manufactured polymer structures," *Polymers*, vol. 12, 1166, 2020. doi: 10.3390/polym12051166

[22] M. A. Yardimci and S. Güceri, "Conceptual framework for the thermal process modelling of fused deposition," *Rapid Prototyp. J.*, vol. 2, no. 2, pp. 26–31, 1996. doi: 10.1108/13552549610732070

[23] S. F. Costa, F. M. Duarte, and J. A. Covas, "Thermal conditions affecting heat transfer in FDM/FFE: A contribution towards the numerical modelling of the process," *Virtual Phys. Prototyp.*, vol. 10, no. 1, pp. 35–46, 2015. doi: 10.1080/17452759.2014.984042

[24] X. Zhou, S. J. Hsieh, and Y. Sun, "Experimental and numerical investigation of the thermal behaviour of polylactic acid during the fused deposition process." *Virtual Phys. Prototyp.*, vol. 12, no. 3, pp. 221–233, 2017. doi: 10.1080/17452759.2017.1306450

[25] A. D'Amico and A. M. Peterson, "An adaptable FEA simulation of material extrusion additive manufacturing heat transfer in 3D," *Addit. Manuf.*, vol. 21, pp. 422–430, 2018. doi: 10.1016/j.addma.2018.02.021

[26] C. Kousiatza and D. Karalekas, "In-situ monitoring of strain and temperature distributions during fused deposition modeling process," *Mater. Des.*, vol. 97, pp. 400–406, 2016. doi: 10.1016/j.matdes.2016.02.099

[27] J. E. Seppala and K. D. Migler, "Infrared thermography of welding zones produced by polymer extrusion additive manufacturing," *Addit. Manuf.*, vol. 12, pp. 71–76, 2016. doi: 10.1016/j.addma.2016.06.007

[28] S. F. Costa, F. M. Duarte, and J. A. Covas, "An analytical solution for heat transfer during deposition in extrusion-based 3D printing techniques," in *Proc. 15th Int. Conf. Comput. Math. Methods Sci. Eng.*, 2015, pp. 1161–1172. doi: 10.13140/RG.2.1.1234.5678

[29] F. Yang and R. Pitchumani, "Healing of thermoplastic polymers at an interface under nonisothermal conditions," *Macromolecules*, vol. 35, pp. 3213–3224, 2002. doi: 10.1021/ma011547t

[30] F. M. Duarte, J. A. Covas, and S. F. Costa, "Predicting the effect of build orientation and process temperatures on the performance of parts made by fused filament fabrication," *Rapid Prototyp. J.*, vol. 28, no. 4, pp. 704–715, 2022. doi: 10.1108/RPJ-06-2021-0156

[31] S. F. Costa, F. M. Duarte, and J. A. Covas, "The effect of a phase change on the temperature evolution during the deposition stage in fused filament fabrication," *Computers*, vol. 10, no. 2,. 19, 2021. doi: 10.3390/computers10020019

[32] S. F. Costa, F. M. Duarte, and J. A. Covas, "Computer aided definition of the printing conditions of parts made by FFF," *Int. J. Mech. Eng. Robot. Res.*, vol. 10, no. 6, pp. 301–307, 2021. doi: 10.18178/ijmerr.10.6.301-307

[33] S. Charlon, J. L. Boterff, and J. Soulestin, "Fused filament fabrication of polypropylene: Influence of the bead temperature on adhesion and porosity," *Addit. Manuf.*, vol. 38, 101838, 2021. doi: 10.1016/j.addma.2020.101838